AIP Journal of Applied Physics

Effective thermal conductivity of particulate composites with interfacial thermal resistance

Ce-Wen Nan, R. Birringer, David R. Clarke, and H. Gleiter

Citation: Journal of Applied Physics **81**, 6692 (1997); doi: 10.1063/1.365209
View online: http://dx.doi.org/10.1063/1.365209
View Table of Contents: http://scitation.aip.org/content/aip/journal/jap/81/10?ver=pdfcov
Published by the AIP Publishing

Effective thermal conductivity of particulate composites with interfacial thermal resistance

Ce-Wen Nan[a)] and R. Birringer
FB 10.3 Technische Physik, Universtät des Saarlandes, D-66041 Saarbrücken, Germany

David R. Clarke
Materials Department, University of California, Santa Barbara, California 93106-5050

H. Gleiter
Forschungszentrum Karlsruhe GmbH, D-76021, Germany

(Received 15 October 1996; accepted for publication 17 February 1997)

A methodology is introduced for predicting the effective thermal conductivity of arbitrary particulate composites with interfacial thermal resistance in terms of an effective medium approach combined with the essential concept of Kapitza thermal contact resistance. Results of the present model are compared to existing models and available experimental results. The proposed approach rediscovers the existing theoretical results for simple limiting cases. The comparisons between the predicted and experimental results of particulate diamond reinforced ZnS matrix and cordierite matrix composites and the particulate SiC reinforced Al matrix composite show good agreement. Numerical calculations of these different sets of composites show very interesting predictions concerning the effects of the particle shape and size and the interfacial thermal resistance. © *1997 American Institute of Physics.* [S0021-8979(97)08010-9]

I. INTRODUCTION

Particulate composites such as ceramic particle reinforced metal matrix composites have been extensively investigated since they are used to many applications from structural materials to electric devices. These particulate composites have been developed in many forms with a variety of different particle sizes, volume fractions, shapes, and topologies that are dependent of the particular processing route used to fabricate the materials. Understanding of the effects of these microstructural characteristics on properties of composite materials has been a topic of considerable theoretical interest (see, for example, Refs. 1–4). In the literature, most works have focused on the idealized case of perfect interface contact. In the present work, the effect of these microstructural parameters on the thermal conductivity of particulate composites with imperfect interfacial thermal contact will be emphasized.

It is known that the interfacial thermal contact resistance between different constituent phases in a composite can arise from the combination of a poor mechanical or chemical adherence at the interface and a thermal expansion mismatch. This interfacial resistance is now known as the Kapitza resistance,[5] R_{Bd}, after Kapitza's discovery[6] of temperature discontinuity at the metal–liquid interface. Many experiments on the thermal conductivity of various composite systems[7–14] have shown that the interfacial thermal resistance has a dramatical effect on the effective thermal conductivity, K^*, of the composites. Although the interfacial effect in the composites has been known recognized for some time, theoretical work on this effect has been performed only recently. The first two theoretical analyses of this problem were conducted by Hasselman and Johnson,[15] and by Benvensite,[16] respectively. Hasselman and Johnson[15] extended the classical work of Maxwell[17] and Lord Rayleigh[18] to consider simply spherical particulate and cylindrical fiber reinforced matrix composites and derived a Maxwell–Garnett type effective medium approximation (EMA) for calculating K^* in which the interface effect and particle size are included. Benvensite also derived the same result based on a micromechanical model. Starting from this Maxwell–Garnett type EMA (MG-EMA), Every *et al.*[11] gave an asymmetric Bruggeman type EMA based on Bruggeman's integration embedding principle.[19] Davis and Artz[20] confirmed the validity of this MG-EMA to predict K^* of such spherical particulate composites by comparing the EMA results with finite-element calculations of axisymmetric unit-cell models. For nonspherical particulate composites, Hatta and Taya[21] and Benveniste and Miloh[22] proposed several analytical models to predict K^* of composites containing aligned or randomly oriented coated short fibers. Along similar lines, Dunn and Taya[23] extended a Mori–Tanaka[24] type analytical approach for coated short-fiber composites to numerically show the effect of the interfacial thermal resistance in slightly nonspherical particulate composites and predicted a very strong dependence of K^* on particle shapes, which is strange and will be discussed later.

Other different line of theoretical investigation is concerned with bounding techniques recently developed by Torquato and Rintoul[25] and Lipton and Vernescu.[26(a)] Torquato and Rintoul[25] proposed tighter bounds on K^* of such spherical particulate composites by using minimum energy principles. Their bounds contain unknown parameters related to higher-order correlation functions. Lipton and Vernescu[26(a)] also derived different bounds whose lower bound contains a so-called formation factor m_0 (i.e., the normalized effective conductivity of the corresponding compos-

[a)]On leave from the Advanced Materials Research Institute, Wuhan University of Technology, Wuhan, Hubei 430070, People's Republic of China. Electronic mail: c.nan@rz.uni-sb.de

ites with the inclusion of particles replaced by voids of the same shape) and is sensitive to the determination of this factor m_0. However, this formation factor can be theoretically determined by using various methods.

An important point to all this theoretical understanding of the interface effect in the particulate composites is prediction of their particle size effect. The purpose of the present article is to develop a more general EMA formulation for the effective thermal conductivity of arbitrary particulate composites with interfacial thermal resistance based on multiple-scattering theory.[27] The article is organized as follows. First, we briefly review the multiple-scattering theory and then a general EMA formulation for arbitrary ellipsoidal particulate composites with interfacial thermal resistance is derived, followed by detailed formulations of several ellipsoidal particle geometry and topologies that rediscover the MG-EMA results derived by several researchers for simple cases. For illustrative and quantitative purposes, numerical results for particulate diamond reinforced ZnS matrix (diamond/ZnS) and cordierite matrix (diamond/cordierite) composites and the particulate SiC reinforced Al matrix (SiC/Al) composite are given and discussed; these results are also compared to existing models and available experimental results.

II. EFFECTIVE MEDIUM THEORY

A. General framework

First we briefly review the multiple-scattering approach following Nan.[4] Let us consider a composite medium whose thermal conductivity varies from point to point. The variation can be expressed in the form: $K(r)=K^0+K'(r)$, where K^0 denotes a constant part of a homogeneous medium and $K'(r)$ is an arbitrary fluctuating part. By using the Green function G (Ref. 28) for the homogeneous medium defined by K^0 and the transition matrix T for the entire composite medium, a rigorous solution for the temperature gradient distribution can be obtained. The resulting effective thermal conductivity K^* of the composite is expressed as

$$K^*=K^0+\langle T\rangle(I+\langle GT\rangle)^{-1}, \tag{1}$$

where I is the unit tensor and $\langle\ \rangle$ denotes spatial averaging. The matrix, T, is

$$T=\sum_n T_n+\sum_{n,m\neq n} T_n G T_m+\ldots, \tag{2}$$

where the first term is the sum of the T matrices of n particles and the successive terms represent the interaction between particles. An accurate calculation of T is a formidable problem. For simplicity of calculation, we approximate T as

$$T\cong\sum_n T_n=\sum_n K_n'(I-GK_n')^{-1}, \tag{3}$$

thereby neglecting interparticle multiple scattering. Obviously, this approximation is only valid when the inclusion particles are dispersed in the matrix.

Now let us consider an ellipsoidal particle in the matrix and its surrounding interface layer of thickness δ and conductivity K_s as a composite unit cell. From Eq. (1), by choosing $K^0=K_s$, we directly obtain the equivalent thermal conductivities, K_{ii}^c $(i=1,2,3)$, along the X_i' symmetric axis of this ellipsoidal composite unit cell as follows

$$K_{ii}^c=K_s\,\frac{K_s+L_{ii}(K_p-K_s)(1-v)+v(K_p-K_s)}{K_s+L_{ii}(K_p-K_s)(1-v)}, \tag{4}$$

with

$$v=a_1{}^2a_3/(a_1+\delta)^2(a_3+\delta),$$

where K_p is the thermal conductivity of the ellipsoidal particle; a_1 and a_3 are, respectively, radii of the ellipsoid along the X_1' and X_3' axes; and L_{ii} are well-known geometrical factors dependent on the particle shape and given by[28]

$$L_{11}=L_{22}=\begin{cases}\dfrac{p^2}{2(p^2-1)}-\dfrac{p}{2(p^2-1)^{3/2}}\cosh^{-1}p, & \text{for } p>1,\\[2ex] \dfrac{p^2}{2(p^2-1)}+\dfrac{p}{2(1-p^2)^{3/2}}\cos^{-1}p, & \text{for } p<1,\end{cases} \tag{5}$$

$$L_{33}=1-2L_{11}, \tag{6}$$

where $p=a_3/a_1$ is the aspect ratio of the ellipsoid, and $p>1$ and $p<1$ are for a prolate $(a_1=a_2<a_3)$ and an oblate $(a_1=a_2>a_3)$ ellipsoidal inclusion, respectively.

By ultimately passing to the limit that $\delta\to 0$ and that $K_s\to 0$, (the interfacial thermal resistance is thought of as the limiting case of heat transport across bulk phase separated by a thin, poorly conducting interphase region), we rewrite Eq. (4) as

$$K_{ii}^c=K_p/(1+\gamma L_{ii}K_p/K_m), \tag{7}$$

with

$$\gamma=\begin{cases}(2+1/p)\alpha, & \text{for } p\geqslant 1\\ (1+2p)\alpha, & \text{for } p\leqslant 1\end{cases}. \tag{8}$$

Here a dimensionless parameter, α, is introduced, and is defined by

$$\alpha=\begin{cases}a_k/a_1, & \text{for } p\geqslant 1,\\ a_k/a_3, & \text{for } p\leqslant 1\end{cases}, \tag{9}$$

in which the interfacial thermal property is concentrated on a surface of zero thickness and characterized by the Kapitza radius, a_k, defined as

$$a_k=R_{Bd}K_m, \quad \text{with } R_{Bd}=\lim_{\substack{\delta\to 0\\ K_s\to 0}}(\delta/K_s), \tag{10}$$

where K_m is the thermal conductivity of the matrix phase.

Generally, $0\leqslant a_k\leqslant\infty$, with $a_k=0$ corresponding to the perfect interface. For $a_k>0$, temperature jumps across the interface. By contrast, for the conductance case where heat flux jumps across the interface, we can also rewrite Eq. (4) as

$$K_{ii}^c=K_p+\gamma(1-L_{ii})K_m. \tag{11}$$

In this case, the dimensionless parameter α in γ [see Eq. (8)] becomes

$$\alpha=\begin{cases}a_c/a_1, & \text{for } p\geqslant 1,\\ a_c/a_3, & \text{for } p\leqslant 1\end{cases}, \tag{12}$$

where

$$a_c=\Sigma_{Bd}/K_m, \quad \text{with } \Sigma_{Bd}=\lim_{\substack{\delta\to 0\\ K_s\to\infty}}(\delta\ K_s). \tag{13}$$

Similarly, $0\leqslant a_c\leqslant\infty$, with $a_c=0$ corresponding to the perfect interface. For brevity, in the present work we focus upon the case of interfacial thermal resistance.

We now consider a two-phase composite containing ellipsoidal inclusions with the interfacial thermal resistance existing between the matrix and inclusions, in which the materials axes are denoted by X_i, and the local, oriented axes by X_i', with X_3' coinciding with the symmetric axis of the inclusion particles considered. From Eq. (1), by taking $K^0=K_m$, we obtain the effective thermal conductivity of the composite with equisized ellipsoidal particles as

$$K_{11}^*=K_{22}^*=K_m\frac{2+f[\beta_{11}(1-L_{11})(1+\langle\cos^2\theta\rangle)+\beta_{33}(1-L_{33})(1-\langle\cos^2\theta\rangle)]}{2-f[\beta_{11}L_{11}(1+\langle\cos^2\theta\rangle)+\beta_{33}L_{33}(1-\langle\cos^2\theta\rangle)]}, \tag{14a}$$

$$K_{33}^*=K_m\frac{1+f[\beta_{11}(1-L_{11})(1-\langle\cos^2\theta\rangle)+\beta_{33}(1-L_{33})\langle\cos^2\theta\rangle]}{1-f[\beta_{11}L_{11}(1-\langle\cos^2\theta\rangle)+\beta_{33}L_{33}\langle\cos^2\theta\rangle]}, \tag{14b}$$

with

$$\beta_{ii}=\frac{K_{ii}^c-K_m}{K_m+L_{ii}(K_{ii}^c-K_m)}, \tag{15}$$

$$\langle\cos^2\theta\rangle=\frac{\int\rho(\theta)\cos^2\theta\sin\theta d\theta}{\int\rho(\theta)\sin\theta d\theta}, \tag{16}$$

where θ is the angle between the materials axis X_3 and the local particle symmetric axis X_3', $\rho(\theta)$ is a distribution function describing ellipsoidal particle orientation, and f is the volume fraction of particles. Equations (14) are general EMA formulations that contain the effects of particle size, shape, orientation distribution, volume fraction, interfacial thermal resistance, and K_p and K_m on K^* of the particulate composites. From Eqs. (14), simplified expressions for K^* can be easily given for several inclusion geometry and topologies.

B. Formulations for four limiting cases of interest

1. Aligned continuous fibers

For continuous fiber composites with uniformly distributed long fibers oriented parallel to the X_3 axis, $p\to\infty$, $L_{11}=0.5$, and $L_{33}=0$, and $\langle\cos^2\theta\rangle=1$, then Eqs. (7) and (14) reduce to

$$\begin{aligned}K_{11}^c&=K_{22}^c=K_p/(1+\alpha K_p/K_m),\\ K_{33}^c&=K_p,\end{aligned} \tag{17}$$

and

$$K_{11}^*=K_{22}^*=K_m\frac{K_p(1+\alpha)+K_m+f[K_p(1-\alpha)-K_m]}{K_p(1+\alpha)+K_m-f[K_p(1-\alpha)-K_m]}, \tag{18a}$$

$$K_{33}^*=(1-f)K_m+fK_p, \tag{18b}$$

respectively. Equation (18a) is identical to Hasselman and Johnson's result[15] and is also a MG-EMA for two-dimensional isotropic composites with circular inclusions. Equation (18b) is the rule of mixture for a simple parallel model.

2. Laminated flat plates

For laminate composites with a matrix containing parallel flat plate inclusions oriented perpendicular to the X_3 axis, $p\to 0$, $L_{11}=0$ and $L_{33}=1$, and $\langle\cos^2\theta\rangle=1$, and thus Eqs. (7) and (14) reduce, respectively, to

$$\begin{aligned}K_{11}^c&=K_{22}^c=K_p,\\ K_{33}^c&=K_p/(1+\alpha K_p/K_m),\end{aligned} \tag{19}$$

and

$$K_{11}^*=K_{22}^*=(1-f)K_m+fK_p, \tag{20a}$$

$$K_{33}^*=K_pK_m/[K_p-f(K_p-K_m-\alpha K_p)]. \tag{20b}$$

Equation (20b) is also identical to Hasselman and Johnson's result.[15]

3. Spheres

When the ellipsoidal inclusions become spheres, $p=1$, $L_{11}=L_{33}=1/3$, and $\langle\cos^2\theta\rangle=1/3$, then Eq. (7) reduces to

$$K_{11}^c=K_{22}^c=K_{33}^c=K_p/(1+\alpha K_p/K_m), \tag{21}$$

and K^* is

$$K^*=K_m\frac{K_p(1+2\alpha)+2K_m+2f[K_p(1-\alpha)-K_m]}{K_p(1+2\alpha)+2K_m-f[K_p(1-\alpha)-K_m]}, \tag{22}$$

which reverts back to the MG-EMA derived by Hasselman and Johnson[15] and by Benvensite.[16]

4. Completely misoriented ellipsoidal particles

In the case of completely random oriented ellipsoidal inclusions, $\langle\cos^2\theta\rangle=1/3$, then K^* of the isotropic composites becomes

$$K^*=K_m\frac{3+f[2\beta_{11}(1-L_{11})+\beta_{33}(1-L_{33})]}{3-f[2\beta_{11}L_{11}+\beta_{33}L_{33}]}, \tag{23}$$

which is a general MG-EMA for arbitrary isotropic particulate composites. Based on this equation, an asymmetric

TABLE I. Thermal properties of materials at room temperature used for the present numerical calculations.

Properties	Diamond/ZnS	SiC/Al	Diamond/ Cordierite
K_p (W/mK)	600	300	600
K_m (W/mK)	17.4	178	4
R_{Bd} (m^2K/W)	6×10^{-8}	6.85×10^{-9}	7×10^{-8}
a_k (μm)	1.044	1.22	0.28

Bruggeman type EMA for such composites is easily obtained by using Bruggeman's integration embedding scheme[4] (not presented here).

III. SOME NUMERICAL RESULTS AND COMPARISON WITH EXPERIMENTS

To illustrate the predictions of the effective medium approach proposed above, we take the diamond/ZnS, (Ref. 11) SiC/Al,[9] and diamond/cordierite[12] composites as examples and compare calculations with the reported effective thermal conductivity of these composites with different particle volume fractions and/or sizes. The pertinent thermal properties at room temperature of each phase used for calculations are given in Table I.

The normalized effective thermal conductivity, K^*/K_m, calculated for the diamond/ZnS composite with spherical dispersions of two different average radii (small particles of $a_{\text{ave}}\approx0.25\ \mu$m and large particles of $a_{\text{ave}}\approx2\ \mu$m) is shown in Fig. 1. Also shown in Fig. 1 are predictions of the asymmetric Bruggeman type EMA[11] and Dunn and Taya's results[23] and Lipton–Vernescu bounds[26] in which two lower bounds are the least lower bounds in the limiting case of $m_0=0$. In the present case, these two different EMAs and Dunn and Taya's approach give very close predictions which lie in the Lipton–Vernescu bounds. The MG-EMA predictions (the same as the Bruggeman type EMA and Dunn and Taya's approach) for the composite containing large particles are in good agreement with the experiment, since the large particles in the composite are largely spherical.[11] However, the predictions for the case of small particles are much higher than the experiment which even lies below the limit of completely insulating interfaces (i.e., $\alpha\rightarrow\infty$). The experimental data are closer to the corresponding Lipton–Vernescu least lower bound. However, if a more reasonable value of m_0, i.e., $m_0>0$, is taken, then the experimental data are also far below this lower bound.[26(a)] This large discrepancy is not due to spatial variations in particle size and interfacial thermal resistance because the limit of $\alpha\rightarrow\infty$ already assumes that the interfaces are totally insulating and that all particles act thermally as voids, rather, it is probably related to the particle shape, as Every *et al.* suggested.[11]

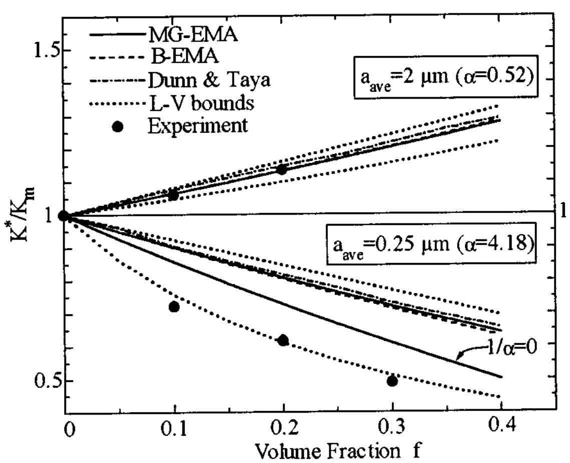

FIG. 1. Comparison between different predictions given using the MG-EMA, asymmetric Bruggeman type EMA (B-EMA), Dunn and Taya's approach, and Lipton–Vernescu ($L-V$) bounds, and experiment (see Ref. 11) for the normalized thermal conductivity K^*/K_m of the spherical particulate diamond/ZnS composite with two different particle radii (or α values) of $a_{\text{ave}}\approx2\ \mu$m ($\alpha=0.52$) above the $1-1$ axis and $a_{\text{ave}}\approx0.25\ \mu$m ($\alpha=4.18$) below the $1-1$ axis. The MG-EMA results in the limiting case of $\alpha\rightarrow\infty(1/\alpha=0)$ are also given. Here Dunn and Taya's results are directly taken from their Figs. 7 and 8 (see Ref. 23) and two Lipton–Vernescu lower bounds are the least lower bounds in the limiting case of $m_0=0$ (see Ref. 26).

The effect of particle shape on K^*/K_m of the isotropic diamond/ZnS composite is shown in Fig. 2 which illustrates that predictions of oblate diamond inclusions [Fig. 2(a)] are consistent with the experiment, and this supports the hypothesis of Every *et al.*[11] Comparison of Fig. 2 and Fig. 1 shows that the predictions on the particle shape effect given by our MG-EMA and by Lipton–Vernescu bounds are totally different from Dunn and Taya's results which is strange. They predicted that slight variations in the particle shape (only from $p=1$ to $p=0.5$ and $p=2$) result in dramatical changes of K^*. For the composite containing slightly oblate particles (only $p=0.5$) of large size ($\alpha=0.52$), they also gave predictions of $K^*/K_m<1$, as they did for the case of small particles ($\alpha=4.18$), which even lie far below the corresponding Lipton–Vernescu least lower bound [Fig. 2(a)]. In the case of small oblate particles ($p=0.5$ and $\alpha=4.18$), their results are close to the corresponding Lipton–Vernescu least lower bound at $f<0.2$ but are also beyond this least lower bound at $f>0.2$. By contrast, for the composite containing slightly prolate particles (only $p=2$), their predictions are around the corresponding Lipton–Vernescu upper bound for the case of small prolate particles ($\alpha=4.18$) but far beyond the corresponding upper bound for the case of large prolate particles ($p=2$ and $\alpha=0.52$), as shown in Fig. 2(b).

For further comparison with reported experiments, we also calculated K^* of SiC/Al and diamond/cordierite composites with different particle sizes (Fig. 3). Figure 3 shows that good agreement between the predicted and experimental data[9,12] of these two different composites is obtained by considering nonspherical inclusions, which reinforces the hypothesis of Hasselman *et al.* Figure 3 also clearly shows the effect of the dimensionless parameter α (Ref. 29) on K^*/K_m which decreases with the rise in α (i.e., the decrease in particle size), especially near a critical dimensionless parameter α^* at which $K^*/K_m=1$. $K^*/K_m>1$ or <1 as $\alpha<\alpha^*$ or $\alpha>\alpha^*$, respectively.

Figure 4 shows more clearly the effects of particle shape on K^*/K_m in two different cases of a large and a small ratio of K_p/K_m. As $\alpha=0$, i.e., no interfacial thermal resistance,

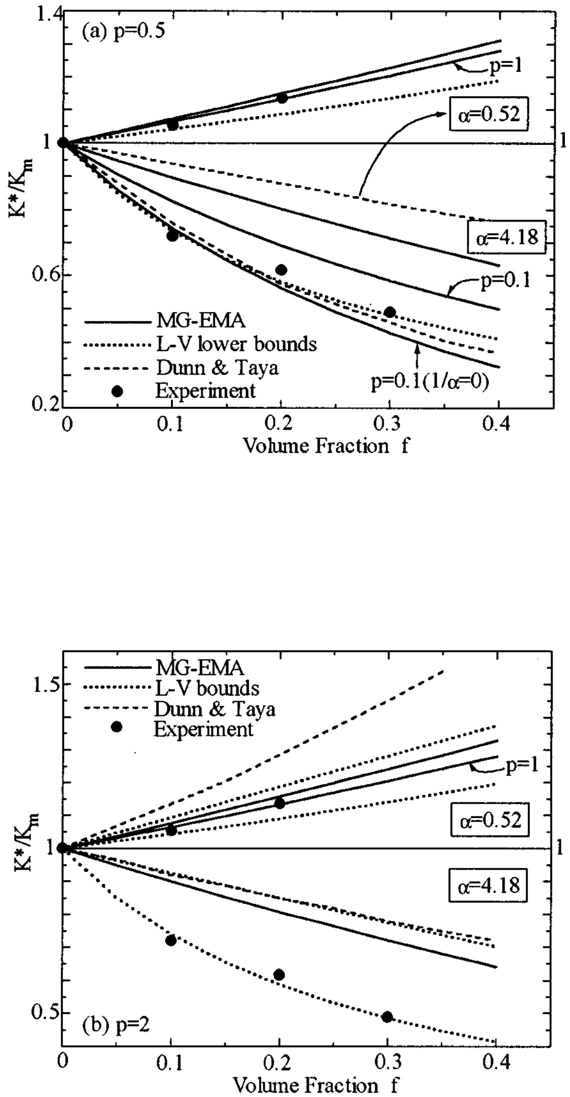

FIG. 2. Comparison between the MG-EMA predictions, numerical results of Dunn and Taya (from their Figs. 7 and 8) (see Ref. 23), Lipton–Vernescu bounds, and experiment (see Ref. 11) for K^*/K_m of the diamond/ZnS composite for two different α values of $\alpha=0.52$ and $\alpha=4.18$, and (a) slightly oblate ($p=0.5$) and (b) prolate ($p=2$) diamond inclusions. For comparison, our MG-EMA results for $p=0.1$ in the cases of $\alpha=4.18$ and $\alpha\rightarrow\infty$ and for $p=1$ in the case of $\alpha=0.52$ are also given. The results for $p=1$ in the case of $\alpha=4.18$ are not shown here because they are very close to those for $p=2$ and $p=0.5$. Here four Lipton–Vernescu lower bounds are also the least lower bounds in the limiting case of $m_0=0$; they move slightly downward in comparison to the least lower bounds for $p=1$ shown in Fig. 1.

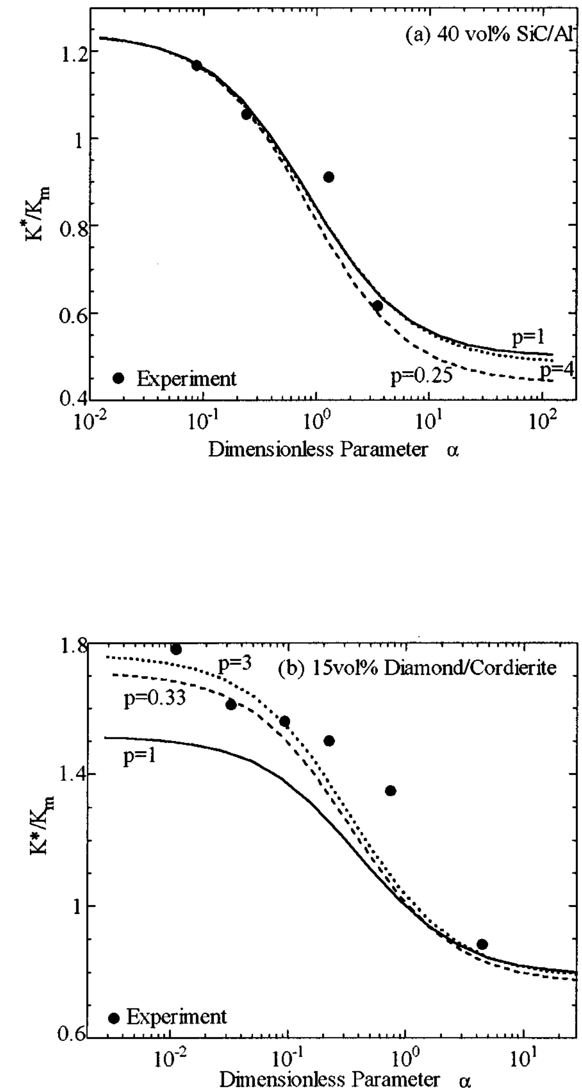

FIG. 3. Comparison between the MG-EMA predictions and experiments (see Refs. 9 and 12) for the effect of the dimensionless parameter α (or particle size) on K^*/K_m of (a) a 40 vol % SiC/Al composite and (b) a 15 vol % diamond/cordierite composite.

K^*/K_m very slightly increases with the anisotropy of the inclusion shape for the case of small K_p/K_m [Figs. 4(b) and 3(a)], whereas K^*/K_m of the composite with large K_p/K_m [Figs. 4(a) and 3(b)] significantly increases with the anisotropy of the inclusion shape. As $\alpha>0$, i.e., considering the interfacial thermal resistance, the effect of p on K^*/K_m becomes more complicated; it also depends on K_p/K_m. For the diamond/ZnS composite with large K_p/K_m, the ellipsoidal inclusions, especially prolate inclusions, are beneficial in increasing K^*/K_m at small α values (e.g., $\alpha<0.5$), as shown in Figs. 4(a) and 3(b). For the SiC/Al composite with small K_p/K_m [Figs. 4(b) and 3(a)], the particle shape has only a slight effect on K^*/K_m at small α values, while at large α values K^*/K_m is always less than 1 no matter what the value of p is.

Figure 5 shows the effect of a uniform orientation distribution $[\rho(\theta)=1]$ between $\theta=0$ and $\theta_{\max}$ of ellipsoidal inclusions on K^*/K_m of the diamond/ZnS and SiC/Al composites. As expected, K_{33}^* decreases and K_{11}^* increases with $\theta_{\max}$ for prolate inclusions, and by contrast, K_{33}^* increases and K_{11}^* decreases with $\theta_{\max}$ for oblate inclusions. The axial principle conductivities $K_{11}^*(=K_{22}^*)$ and K_{33}^* of the diamond/ZnS composite with large K_p/K_m are more sensitive to the distribution cutoff angle $\theta_{\max}$ than those of the SiC/Al composite with small K_p/K_m.

IV. DISCUSSION

Generally, the effective thermal conductivity K^* of a composite, not taking the interface effect into account, lies

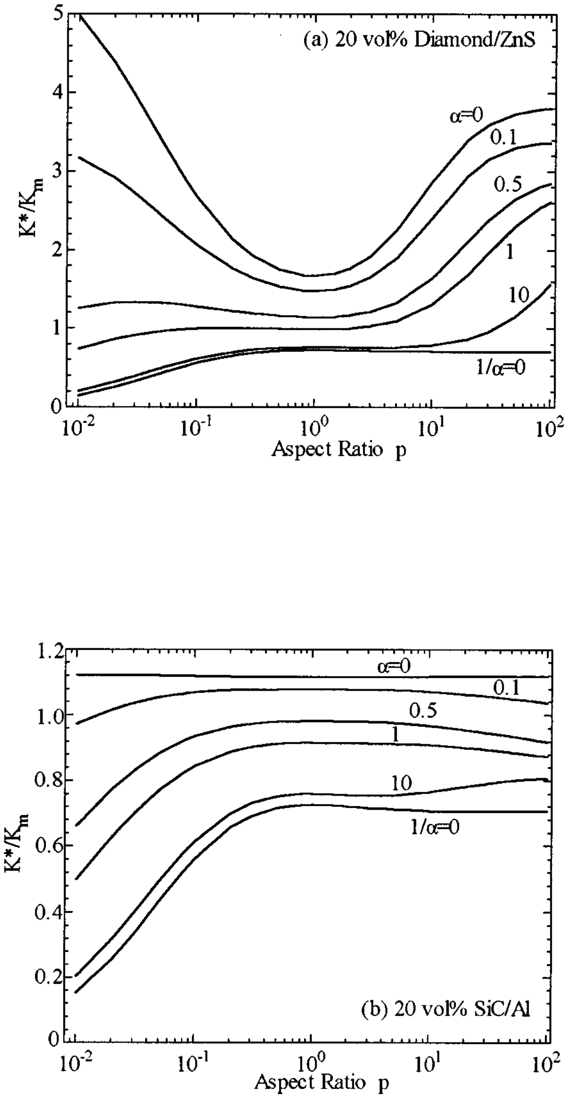

FIG. 4. The effect of the aspect ratio p of the ellipsoidal inclusions on K^*/K_m of (a) a 20 vol % diamond/ZnS composite and (b) a 20 vol % SiC/Al composite for different α values.

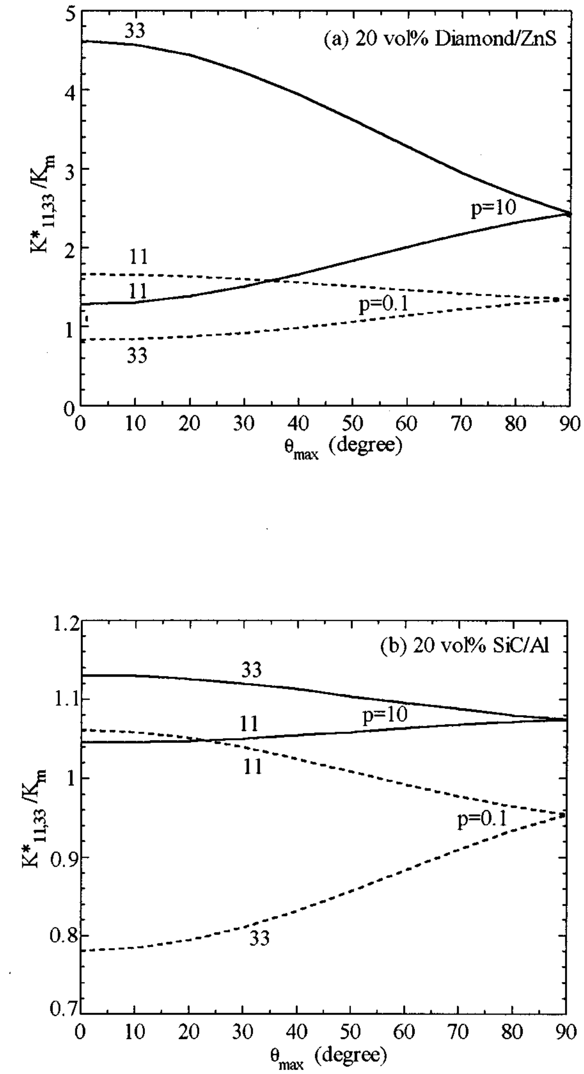

FIG. 5. The effect of the orientation of ellipsoidal inclusions on K_{11}^*/K_m and K_{33}^*/K_m of (a) a 20 vol % diamond/ZnS composite and (b) a 20 vol % SiC/Al composite for $\alpha=0.2$. A uniform orientation distribution between $\theta=0$ and $\theta_{\max}$ is assumed, i.e., $\rho(\theta)=1$.

between the bounds limited by the thermal conductivities of its constituent phases. However, when considering the interfacial thermal resistance, K^* may be beyond the bounds. This is also true for other properties of the composites. A number of reported results has proved that the EMA is a simple and powerful approach in describing the essential properties of composites with a perfect interface. For composites with imperfect interfaces, actually, the EMA is also simple and useful. The MG-EMA calculations in this work reveal a variety of behaviors of composites with interfacial thermal resistance, and demonstrate that K^* is significantly altered by interfacial thermal resistance and by the particle shape and size aside from particle volume fraction and relative thermal conductivity ratio K_p/K_m.

The comparison of the MG-EMA predictions with experimental results of three different composites shows good agreement after considering the particle shape. In a given particle concentration and with perfect interfacial thermal contact between the matrix and inclusions ($a_k=0$), ellipsoidal inclusions with high thermal conductivity result in an obvious enhancement effect in K^* since ellipsoidal inclusions more easily form a path for heat flow through the composite, which is not provided by the same amount of spherical inclusions. By contrast, in the limiting case of inclusions acting as voids ($a_k\rightarrow\infty$), ellipsoidal inclusions, especially oblate inclusions, result in a decrease in K^* that is more pronounced than the decrease caused by spherical particles because oblate inclusions more easily form thermally insulating barriers to the heat flow.

When there is interfacial thermal resistance ($0<a_k<\infty$), K^* of the composite is dependent upon the particle shape in a more complicated way. The complex variations of K^*/K_m with p (Figs. 2–5) are due to changes in the critical dimensionless parameter α^* with p. From Eqs. (14), α^* is determined by

$$\sum_{i=1}^{3}\frac{(K_p/K_m)[1-L_{ii}(2+1/p)p^{1/3}\alpha^*]-1}{L_{ii}(K_p/K_m)[1+(1-L_{ii})(2+1/p)p^{1/3}\alpha^*]+1-L_{ii}}=0. \tag{24}$$

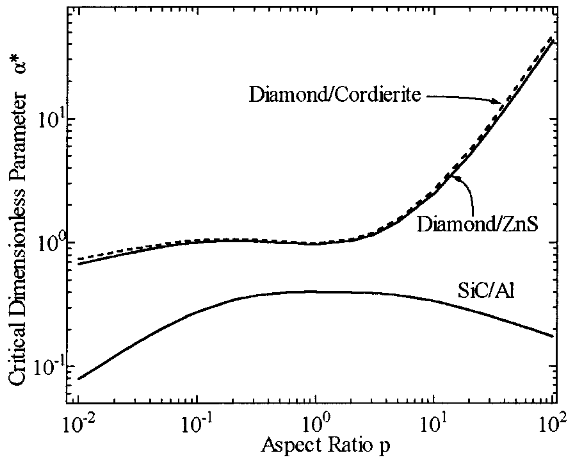

FIG. 6. The critical dimensionless parameter α^* as a function of aspect ratio p for these three different systems: diamond/ZnS, diamond/cordierite, and SiC/Al.

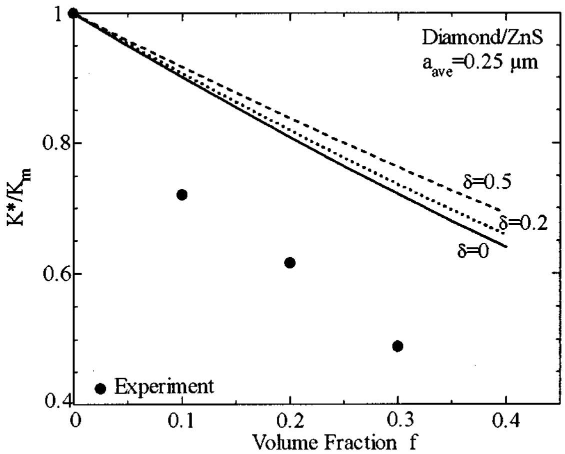

FIG. 7. The effect of the standard deviation δ of the log–normal particle radius distribution on K^*/K_m of the spherical particulate diamond/ZnS composite with small particle sizes distributed over $a = 0.05–0.5$ μm (see Ref. 11).

This critical parameter α^* is dependent on both the particle shape and K_p/K_m. The different systems have totally different α^*, as shown in Fig. 6. For the diamond/ZnS and diamond/cordierite composites with large K_p/K_m, α^* varies slightly with p as $p<3$ and then sharply increases with p as $p>3$. For the SiC/Al composite with small K_p/K_m, α^* always decreases with the increase in inclusion shape anisotropy, especially as $p<0.1$ and $p>10$. A large α^* value easily satisfies $\alpha<\alpha^*$ and results in the increase in K^*, as in the diamond/ZnS composite with prolate inclusions [Fig. 2(b)] and, vice versa, a small α^* value easily satisfies $\alpha > \alpha^*$ and results in decreasing K^* to below K_m, as in the diamond/ZnS composite with oblate inclusions [Fig. 2(a)] and the SiC/Al composite [Figs. 3(a) and 4(b)].

α^* is therefore a very important critical quantity for the composites. Near α^* (or the critical particle size), K^*/K_m dramatically changes (Fig. 3). When $\alpha \gg \alpha^*$, the thermal barrier interface screens the effect of inclusions, whereas when $\alpha \ll \alpha^*$, the thermal resistance interface is not sufficient to form a high thermal barrier. What is more important is that the values of α^* also provide a guideline for tailoring the thermal conductivity of such composites. For example, maximizing the thermal conductivity of a composite is an important criterion in the development of a composite for electronic packaging applications in order to avoid excessive temperature buildup. In order to weaken the effect of the interfacial thermal resistance and to enhance K^* of a composite, α of the composite has to be much less than its α^*. For composites with large K_p/K_m, like the diamond/ZnS and diamond/cordierite composites, it is efficient to enhance K^* by reinforcing the matrix with prolate inclusions (e.g., short fibers or whiskers), while for the composites with small K_p/K_m, like the SiC/Al composite, it is better to reinforce the matrix by using inclusions with p of around 1 to enhance K^*. In this case, α^* cannot be altered by p (Fig. 6). The only way to make $\alpha \ll \alpha^*$ in a given a_k is to increase the particle size. But, on the other hand, larger particles also increase the possibility of particle fracture during processing and performance. Therefore, taking both these effects into consideration for the design of a composite with the desired thermal and mechanical properties is of great importance.

Although uniform particle size and interfacial thermal resistance are assumed in the calculations above, the effect of spatial variations in both particle size and interfacial thermal resistance can be easily evaluated by including the volume average of all possible particle radii and thermal resistances in Eq. (1). For example, by assuming a uniform particle size but a spatial distribution for the Kapitz radius a_k such as Gaussian distribution, it is easy to numerically show that variations in a_k only result in slightly decreasing K^*/K_m of the diamond/ZnS composite (not presented here). As shown in Fig. 1, even the results in the limiting case of $\alpha \rightarrow \infty$ do not, in fact, differ greatly from those for $\alpha = 4.18$. Also, by using a common log–normal distribution function for particle sizes and assuming a uniform interfacial thermal resistance, we can also estimate the effect of particle size distribution on K^*/K_m (Fig. 7). In contrast to a_k variations, particle size variations result in slightly increasing K^*/K_m of the composite.

In this work we have performed only the simple MG-EMA formulations and calculations for composites with Kapitza type interfacial thermal resistance. This work can, however, be extended further to other important cases. The first is calculations of K^* of composites with the interfacial thermal conductance defined by Eqs. (11)–(13) using the same procedure as above. Second, composites with a finite thickness of interface layer or interphase (resistance or conductance), like composites with coated reinforcements,[21–23] can be modeled by starting from Eq. (4). Third, in the derivation of the MG-EMA in Sec. II, we have taken a first-order approximation of the T matrix, Eq. (3), and ignored the interaction between particles, which is known and is available for the case of low inclusion concentration. At high concentration, the multiple interactions between particles must be considered, i.e., one needs to calculate Eq. (3). Finally, the proposed approach can be also generalized to treat any other physical transport properties modeled by Laplace's equation, such as electrostatic problems in composites with interfacial resistance or conductance.

V. CONCLUDING REMARKS

A simple calculational procedure for predicting the effective thermal conductivity of composites made up of arbitrary ellipsoidal inclusions embedded in a matrix with an imperfect matrix-inclusion interface characterized by a Kapitza type interfacial thermal resistance was developed in terms of an effective medium approach combined with Kapitza's thermal contact resistance concept. The comparisons of our numerical results with reported experimental data for diamond/ZnS, SiC/Al, and diamond/cordierite composites show good agreement and reveal that our approach can predict the behavior of effective thermal conductivity of real composites. The present model accounts for properties of the matrix and reinforcement, particle size and size distribution, volume fraction, and interfacial thermal resistance; the effect of the shape and of the orientation of inclusions on the thermal conductivity of the composites, is in particular, successfully accounted for. This work can be further generalized to treat any physical transport properties modeled by Laplace's equation of composites with any imperfect interface and/or interphase.

ACKNOWLEDGMENTS

This work was supported by the State Education Commission of China through the Trans-Century Training Programme Foundation for the Talents (C.W.N.) and by the Alexander von Humboldt Foundation (C.W.N.).

[1] Z. Hashin, J. Appl. Mech. **50**, 481 (1983).
[2] S. Torquato, Appl. Mech. Rev. **44**, 37 (1991).
[3] D. J. Bergman and D. Stroud, Solid State Phys. **46**, 147 (1992).
[4] C.-W. Nan, Prog. Mater. Sci. **37**, 1 (1993).
[5] E. T. Swartz and R. O. Pohl, Rev. Mod. Phys. **61**, 605 (1989).
[6] P. L. Kapitza, J. Phys. (Moscow) **4**, 181 (1941).
[7] H. Bhatt, K. Y. Donaldson, D. P. H. Hasselman, and R. T. Bhatt, J. Am. Ceram. Soc. **73**, 312 (1990).
[8] D. P. H. Hasselman, A. Venkateswaran, M. Yu, and H. Tawil, J. Am. Ceram. Soc. **74**, 1631 (1991).
[9] D. P. H. Hasselman, K. Y. Donaldson, and A. L. Geiger, J. Am. Ceram. Soc. **75**, 3137 (1992).
[10] A. L. Geiger, D. P. H. Hasselman, and K. Y. Donaldson, J. Mater. Sci. Lett. **12**, 420 (1993).
[11] A. G. Every, Y. Tzou, D. P. H. Hasselman, and R. Raj, Acta Metall. Mater. **40**, 123 (1992).
[12] D. P. H. Hasselman, K. Y. Donaldson, J. Liu, L. J. Gauckler, and P. D. Ownby, J. Am. Ceram. Soc. **77**, 1757 (1994).
[13] D. P. H. Hasselman, K. Y. Donaldson, J. R. Thomas, Jr., and J. J. Brennan, J. Am. Ceram. Soc. **79**, 742 (1996).
[14] D. M. Liu and W. H. Tuan, Acta Metall. Mater. **44**, 813 (1996).
[15] D. P. H. Hasselman and L. F. Johnson, J. Compos. Mater. **21**, 508 (1987).
[16] Y. Benvensite, J. Appl. Phys. **61**, 2840 (1987).
[17] J. C. Maxwell (Pergamon, Oxford, 1904), Vol. 1.
[18] Lord Rayleigh, Philos. Mag. **34**, 481 (1892).
[19] D. A. G. Bruggeman, Ann. Phys. (Leipeig), **24**, 636 (1935).
[20] L. C. Davis and B. E. Artz, J. Appl. Phys. **77**, 4954 (1995).
[21] H. Hatta and M. Taya, J. Appl. Phys. **59**, 1851 (1986).
[22] Y. Benveniste and T. Miloh, Int. J. Eng. Sci. **24**, 1537 (1986); J. Appl. Phys. **69**, 1337 (1991).
[23] M. L. Dunn and M. Taya, J. Appl. Phys. **73**, 1711 (1993).
[24] T. Mori and K. Tanaka, Acta. Metall. **21**, 571 (1973).
[25] S. Torquato and M. D. Rintoul, Phys. Rev. Lett. **75**, 4067 (1995).
[26] (a) R. Lipton and B. Vernescu, Proc. R. Soc. London, Ser. A **452**, 329 (1996); (b) J. Appl. Phys. **79**, 8964 (1996).
[27] J. E. Gubernatis and J. A. Krumhansl, J. Appl. Phys. **46**, 1875 (1975).
[28] C.-W. Nan, J. Appl. Phys. **76**, 1155 (1994).

[29] For comparison, in the present calculations we use a unified dimensionless parameter α defined by $\alpha = a_k/a$ where a is the radius of an equivalent spherical particle having the same volume as the ellipsoidal one under consideration, i.e., $a^3 = a_1^2 a_3$.